Biophysical Journal Volume 103 July 2012 38–47

Dynamic Force Spectroscopy on Supported Lipid Bilayers: Effect of Temperature and Sample Preparation

Andrea Alessandrini,[†‡*] Heiko M. Seeger,[†] Tommaso Caramaschi,[‡] and Paolo Facci[†]
[†]Centro S3, CNR-Istituto Nanoscienze and [‡]Department of Physics, University of Modena and Reggio Emilia, Modena, Italy

ABSTRACT Biological membranes are constantly exposed to forces. The stress-strain relation in membranes determines the behavior of many integral membrane proteins or other membrane related-proteins that show a mechanosensitive behavior. Here, we studied by force spectroscopy the behavior of supported lipid bilayers (SLBs) subjected to forces perpendicular to their plane. We measured the lipid bilayer mechanical properties and the force required for the punch-through event characteristic of atomic force spectroscopy on SLBs as a function of the interleaflet coupling. We found that for an uncoupled bilayer, the overall tip penetration occurs sequentially through the two leaflets, giving rise to two penetration events. In the case of a bilayer with coupled leaflets, penetration of the atomic force microscope tip always occurred in a single step. Considering the dependence of the jump-through force value on the tip speed, we also studied the process in the context of dynamic force spectroscopy (DFS). We performed DFS experiments by changing the temperature and cantilever spring constant, and analyzed the results in the context of the developed theories for DFS. We found that experiments performed at different temperatures and with different cantilever spring constants enabled a more effective comparison of experimental data with theory in comparison with previously published data.

INTRODUCTION

Supported lipid bilayers (SLBs) are biological model membranes that constitute suitable systems for both fundamental and technological studies (1–3). In particular, they can be studied by many surface-sensitive techniques, such as ellipsometry, waveguide spectroscopies, x-ray and neutron reflectivity, and atomic force microscopy (AFM) (1). Among these techniques, AFM allows one to perform imaging and force spectroscopy analysis (4,5) simultaneously on a given area. In the framework of SLBs, the force spectroscopy technique is exploited to probe both the mechanical properties of the bilayer at the nanoscale in terms of elastic constants (6) and the force at which the tip, pressing on the membrane, punches through the bilayer by a collapsing mechanism (7–9). It was recently shown that the punch-through force value is related to the temperature of the lipid bilayer (4,10). The process of tip penetration is indeed favored by fluctuations in the bilayer. Ideally, the punch-through phenomenon can be assimilated to a two-state reaction in which the initial state is represented by the tip in contact with the bilayer, and the final one is given by the tip in contact with the substrate (11,12). The penetration process may depend on the internal structure of the lipid bilayer, such as the degree of coupling between the two leaflets. In this context, it would be interesting to relate the features of the tip penetration process to the internal organization of the bilayer. Moreover, the reaction at issue is controlled by the application of a force and, as such, it may depend on the rate of force application. On the basis of this consideration, it would be interesting to study the stress-strain relation of lipid bilayers at different indenting tip speeds. Such an analysis could help elucidate how a lipid bilayer responds to forces applied at different rates. At the same time, because of the correlation between punch-through experiments performed at different tip speeds and the more general area of dynamic force spectroscopy (DFS), the theories developed to interpret DFS experimental data could be tentatively exploited to reconstruct the energy landscape for the punch-through process (13,14). The inferred parameters could be compared with the typical features obtained for the analogous processes of pore formation or fusion in lipid bilayers (15,16).

Several experimental works have shown that in certain aspects, SLBs may exhibit a different behavior with respect to unsupported lipid bilayers (17,18). This difference has been attributed mainly to the strong asymmetry between the two leaflets induced by the presence of the solid substrate in the neighborhood of the proximal leaflet (i.e., that nearer to the substrate), with the distal one (the leaflet facing the bulk aqueous solution) being influenced to a smaller extent by the presence of a substrate (19,20). The asymmetry of the two leaflets could affect the degree of their coupling, the mechanism of which is currently the focus of many experimental and theoretical studies (21,22). Moreover, the interleaflet coupling could also determine how a lipid bilayer reacts to a deformation stimulus applied to either of the two leaflets. It has been demonstrated that, depending on the specific preparation conditions used for the SLB, two phase transitions from the liquid disordered to the solid ordered phase can be observed. The preserved memory of the preparation conditions is related to the deposited number of lipids, which is affected by their area per lipid and consequently by the temperature. The two transitions can

Submitted March 16, 2012, and accepted for publication May 24, 2012.
*Correspondence: andrea.alessandrini@unimore.it
Editor: Peter Hinterdorfer.

0006-3495/12/07/0038/10 $2.00
doi: 10.1016/j.bpj.2012.05.039

be attributed to the independent behavior of the two uncoupled leaflets (18,23) or to an interdigitation effect of the two leaflets at high temperature (24). At the same time, it is possible to prepare SLBs that show only one transition, with the two coupled leaflets presenting in register domains. When a force is applied to an SLB by an AFM tip, the reaction of the bilayer can be affected by the degree of coupling of the two leaflets, and in turn, the degree of the eventually induced coupling will depend on the speed of the indenting tip.

If the punch-through process is described as a mechano-chemical reaction whose energy landscape is characterized by two equilibrium states (the tip on top of the bilayer and the tip in contact with the underlying solid substrate) separated by an energy barrier, we can assume that the effect of an applied force is equivalent to a reduction of the reaction activation energy (13). As a consequence, the rate of escape from the initial equilibrium state will increase with the applied force. If we could quantitatively relate the decrease of energy barrier to the applied force, we could obtain the dependence of the process rate as a function of force. These considerations were developed in a pioneering series of articles in which both a continuum nucleation model based on the analogy with the pore formation process in lipid bilayers and a molecular model were discussed (11,12,25). The two models, fitted to experimental data, can provide estimates for the thermodynamic parameters of the punch-through event. Experimental data involve both the distribution of forces for the rupture process at a given tip speed and the dependence of a statistical parameter of the distributions (typically the most probable force or the average force) obtained for different tip speeds. In the analogous context of DFS, previous investigators obtained the rate of escape from a potential well using the Bell-Evans phenomenological model (13,26), by quantifying the decrease of the activation energy with force as the product of the force and the distance of the transition state from the initial equilibrium state along the pulling coordinate. In this model, if the force is increased linearly with time according to the relation $F = kvt$ (where k is the elastic constant of the cantilever, v is the tip speed, and t is the time (kv is the loading rate)), a plot of the most probable force required to cross the barrier as a function of $log\ v$ will result in a linear trend (14). However, for some systems, it has been found experimentally that the relation between the most probable force and speed does not increase logarithmically as expected (27). The reason for this behavior is unclear. In some cases, the existence of two barriers has been evoked to explain experimental results in which two different linear trends have been obtained in the most-probable-rupture-force versus $log\ v$ plot (28). In other cases, the nonlinear behavior has been interpreted as an evidence of the inadequacy of the Bell-Evans model to describe the complete dynamic range of the reaction mechanism (27). As a result, more sophisticated models, such as the Dudko-Hummer-Szabo (DHS) model, have been introduced. The Bell-Evans model represents a particular case that is valid in a limited range of force increase rates (29–31).

In this work, we studied by force spectroscopy the punch-through event across an SLB as a function of its preparation conditions and temperature. This analysis allowed us to establish the role of the interleaflet coupling in the mechanical properties of lipid bilayers. The punch-through process studied as a function of indentation speed prompted us to use different theoretical models in an attempt to extract thermodynamical parameters for the punch-through phenomenon. The combination of DFS with changing temperature and the use of cantilevers with different spring constants also allowed us to simulate the extension of the probed tip speed range. This strategy serves to improve the data analysis for this kind of experiment. In fact, a limiting aspect of DFS is that the experimentally investigated tip speed range is usually too narrow to allow a meaningful fit of the different theories to data.

MATERIALS AND METHODS

Lipid preparation

The lipids 1-palmitoyl-2-oleoyl-*sn*-glycero-3-phosphoethanolamine (POPE) and 1-palmitoyl-2-oleoyl-*sn*-glycero-3-[phospho-rac-(1-glycerol)] (sodium salt) (POPG) were purchased from Avanti Polar Lipids (Alabaster, AL) and used without further purification. Chloroform was evaporated under a flow of nitrogen while it was heated in a water bath at 50°C. Thereafter, the sample was kept under vacuum (10^{-2} mbar) for at least 4 h to remove the remaining chloroform molecules. Lipids were rehydrated in a buffer solution of 450 mM KCl, 25 mM Hepes at pH 7 to obtain a concentration of 0.25 mg/ml. The sample was sonicated at room temperature in an ultrasonic bath for 15 min, resulting in a homogeneous lipid suspension.

SLB preparation

SLBs were prepared by the vesicle fusion technique as described previously (4). Briefly, 70–100 μl of the lipid suspension were deposited onto a freshly cleaved piece of mica (SPI Supplies/Structure Probe) that was fixed on a Teflon disc attached to a metal disc. The lipid suspension was incubated for 15 min at the temperature of interest and then the sample was subjected to extensive rinsing in the incubation buffer, followed by rinsing with the imaging buffer. For the unsupported POPG and POPE bilayers, the main phase transition occurs at −4°C and 19°C, respectively, at neutral pH. Due to the presence of the substrate, the transition temperatures are shifted to higher values (18). In previous works, we discussed the peculiarities of SLBs relative to the particular aspects of the main phase transition temperature and interleaflet coupling (18,32). In addition to the inherent interleaflet coupling, the presence of the support and its interaction with the proximal leaflet lead to a complex system of forces that affect the coupling (33). In the literature, the interleaflet coupling has been related to the degree of asymmetry in the lipid density between the two layers (34). The stronger the asymmetry (the proximal leaflet has a lipid density higher than the distal one), the weaker the coupling of the two leaflets. In supported POPG and POPE bilayers in distilled water, the two leaflets are uncoupled (18), i.e., they behave independently. When the ionic strength of the solution and the incubation temperature of the bilayer are increased, the interleaflet coupling increases until the temperature-induced phase transition occurs with the two leaflets displaying domains in register (18). Hence, depending on the preparation procedure used for the SLBs, one can have bilayers with coupled or uncoupled leaflets.

Force spectroscopy measurements

Force spectroscopy experiments were performed with a Bioscope microscope equipped with a Nanoscope IIIA controller (Bruker, Santa Barbara, CA). We used a temperature-controlled stage based on a circulating water bath on which we could mount the Bioscope head. The sample temperature was continuously monitored by a digital thermometer Fluke 16 (Fluke, Italy) equipped with a small K-thermocouple probe (Thermocoax GmbH, Germany) in direct contact with the imaging buffer. The stability of the temperature was ensured in the range of $\pm 0.3^{\circ}$C of the specified temperature value. Triangular silicon nitride cantilevers (Bruker DNP-S) with nominal spring constants of 0.06 N/m and 0.24 N/m were used. We determined the elastic constants used to convert deflections into forces by using the thermal noise approach (35). For each investigated tip speed, we acquired >250 force curves with 1024 points. More details about the force-curve acquisition procedure and the force-curve analysis are provided in the Supporting Material.

RESULTS

Force spectroscopy on SLBs with different degrees of interleaflet uncoupling

As a first step, we measured the punch-through force for a POPE supported bilayer as a function of the preparation temperature. We used two temperatures (15°C and 30°C) that allowed us to obtain lipid bilayers with uncoupled and coupled leaflets, respectively (18,31). We performed the force spectroscopy measurements at 25°C in 50 mM KCl solution. For samples prepared at 15°C, tip penetration occurred in two steps, as shown in Fig. 1 *a*. The presence of double jumps in force spectroscopy on SLB has already been reported in the literature (25,36). However, in those cases, the second jump was attributed to the presence of a lipid monolayer/bilayer on the tip. Here, we provide evidence that the two jumps result from the sequential penetration of the two leaflets by the tip. When force spectroscopy measurements were performed on bilayers prepared at 30°C, tip penetration occurred in just one step, as shown in Fig. 1 *b*. We also performed force spectroscopy measurements on POPG supported bilayers prepared in the two limiting situations of uncoupled and coupled leaflets. We again obtained the two above-mentioned features of the punch-through phenomenon. As an example, Fig. 1 *c* shows a force curve obtained on an uncoupled POPG bilayer in distilled water. Here, the presence of two punch-through phenomena highly separated in the corresponding force values is evident (see Fig. S2). When a POPG bilayer is prepared at 20°C and the force curves are measured in 50 mM KCl solution, a different behavior is observed (Fig. 1 *d*). At tip speeds $<$ 600 nm/s, two punch-through events are observed (Fig. 1 *d*, *left*). In this case, the force value separation between the two punch-through events is smaller than the case of Fig. 1 *c* (see Fig. S2). Instead, at tip speeds $>$ 600 nm/s, the punch-through event occurs in only one step (Fig. 1 *d*, *right*). The tip penetration distance in the latter case is almost twice the distance of each single penetration step in the uncoupled leaflet. It should be stressed that this situation is completely reversible. By changing the tip speed, one can switch back and forth over the two situations. The observed behavior points to a possible independent sliding of the two leaflets induced by the indenting tip. In fact, the single-step punch-through mechanism at high tip speed shown in Fig. 1 *d* (*right*) could be the result of an increased friction between the two leaflets

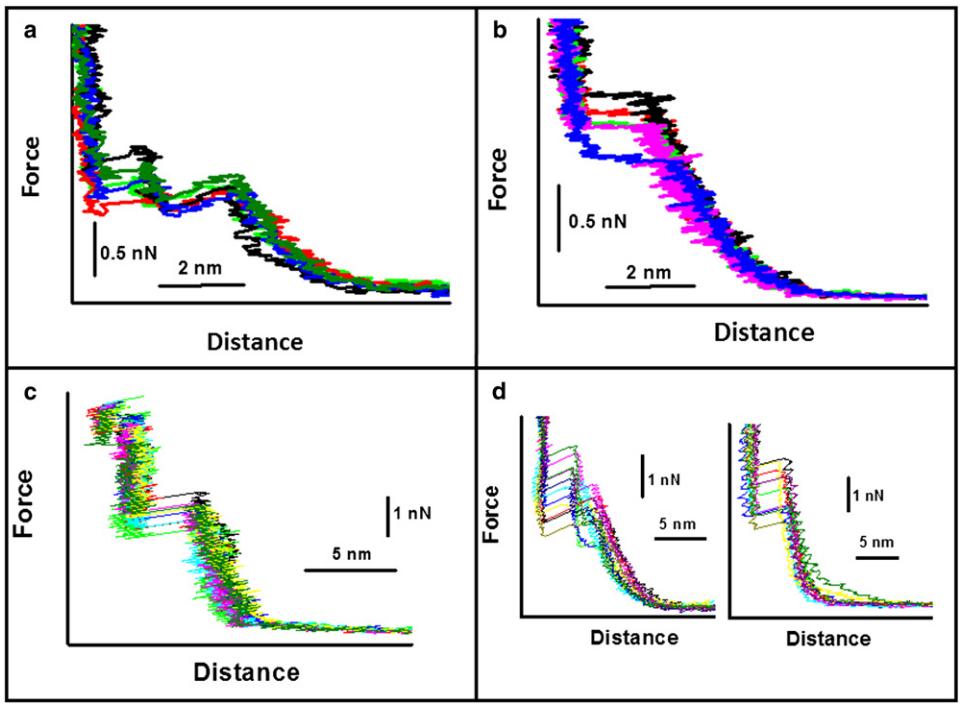

FIGURE 1 (*a*) Force curves obtained on an uncoupled supported POPE bilayer prepared at 15°C. (*b*) Force curves obtained on a coupled POPE supported bilayer prepared at 30°C. (*c*) Force curves obtained on an uncoupled POPG bilayer prepared at 15°C. (*d*) Force curves obtained on a POPG bilayer prepared at 20°C for tip speeds of 359 nm/s (*left*) and 930 nm/s (*right*). Cantilever spring constant: 0.08 $\pm$ 0.2 N/m.

inhibiting the slipping of the distal leaflet on the proximal one (see Supporting Material); thus, penetration would occur only after both leaflets are modified by the tip. The friction here is attributed to a sort of epitactic coupling induced by interdigitation of the lipid alkyl chains (34). Moreover, when two punch-through processes are present, the degree of interleaflet coupling can be related to the separation of the force values corresponding to the two events.

In some cases, the appearance of one or two punch-through processes in the force curves depends on the temperature. In Fig. 2 *a*, a series of force curves obtained on a POPG supported bilayer prepared at 22°C is reported. The sequence was obtained at 27°C in 50 mM KCl with a tip speed of 598 nm/s. The curves show that the penetration through the bilayer occurs in a single step. The penetration distance of ~5 nm is consistent with the thickness of one bilayer. The same feature is observed for all of the investigated tip speeds (from 598 nm/s to 1200 nm/s). Fig. 2 *b* reports a typical distribution of jump-through force values for force curves obtained in the above conditions. By decreasing the temperature to 24°C, the phase transition region for the proximal leaflet is approached. If force curves are measured at this temperature, two possible scenarios are present. In some cases, penetration occurs just in one step, whereas in other cases it occurs in two steps (Fig. 2 *c*). We stress that the bilayer at 24°C is near its phase transition, and it is possible that fluctuations in the bilayer continuously shift the membrane from a coupled to an uncoupled state. Remarkably, the most probable jump-through force value in the case of the single step is about twice the value obtained for the first event in cases where two of them are present, as can be seen from the jump-through force values distribution shown in Fig. 2 *d*. Even in this case, the same behavior is observed for all of the investigated tip speeds. In addition, considering one specific speed value, as shown in Fig. 2 *c*, the force curves that display two steps show a higher repulsive force contribution (before tip-bilayer contact) than those with only one step (*arrow* in Fig. 2 *c*). This effect could be related to the increased electric fields experienced by the tip on the supported bilayer. The increased electric field could be a consequence of the increased local lipid density upon a transition to a solid ordered phase.

DFS as a function of temperature and cantilever spring constant

Considering the process of the AFM tip punch-through as an activated and stochastic reaction, it is possible to extract kinetic information about the rupture event by performing experiments at different tip speeds. We therefore performed DFS measurements on SLBs in different conditions. Attempts to reconstruct the energy landscape by exploiting DFS are complicated by the limited tip speed range that can be experimentally explored without introducing artifacts. To circumvent this limitation as much as possible, we performed experiments at different tip speeds on samples at different temperatures and using cantilevers with different spring constants. This approach allowed us to change the relative mechanical properties between the

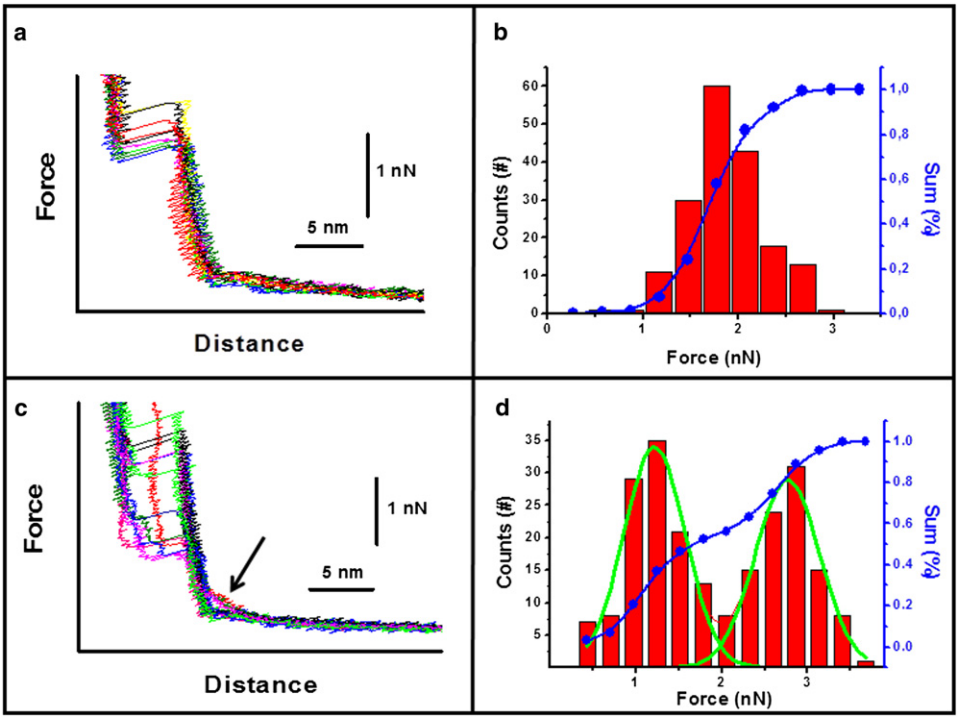

FIGURE 2 (*a*) Force curves obtained on a POPG bilayer at 27°C and tip speed of 598 nm/s. (*b*) Jump-through force values distribution corresponding to the case in panel *a*. (*c*) Force curves obtained on the same POPG bilayer as in panel *a*, but at 24°C. The arrow points to the region of the force curves in which the electrostatic interaction is increased. (*d*) Jump-through force values distribution corresponding to the case in panel *c*.

cantilever and the sample, and thus increased the possibility of observing different regimes in the force versus *log v* characteristics.

We assembled a POPE bilayer with coupled leaflets on a mica substrate by incubating the sample at 35°C. Fig. 3 reports the dependence of the most probable punch-through force value on tip speed for three temperatures: 27°C, 34°C, and 38°C. In these experiments, tip penetration never occurred in two steps, in agreement with the fact that the two leaflets are coupled. Considering the punch-through force values for the different temperatures, we observed a significant decrease from 34°C to 27°C after an increase from 38°C to 34°C. The decrease was due to the lipid bilayer being in the phase transition region at 27°C, as confirmed by AFM imaging (4). The trend of the most probable punch-through force versus *log*(tip speed) depends on temperature. At 38°C, we found an overall linear increase of the force with *log*(tip speed). At 34°C, when the bilayer was still in the liquid-disordered phase, we observed a linear trend for low tip speeds, followed by a steeper trend for higher tip speeds. At 27°C, the bilayer was in the phase transition region and the trend was again linear. These results imply that, given the temperature of the bilayer and consequently its mechanical properties (37), the possibility of observing a deviation from the linear trend in the plot depends on the investigated tip speed range. This means that the values of the mechanical parameters of the sample may determine the transition between different regimes in DFS measurements (29,30).

Fig. 4 reports, for a constant tip speed of 1200 nm/s, three representative force curves, each of which results from averaging over 200 force curves obtained at three different temperatures on the POPE supported bilayer. The inset to the figure shows an AFM image of the POPE bilayer with a defect that allows us to measure the height of the bilayer.

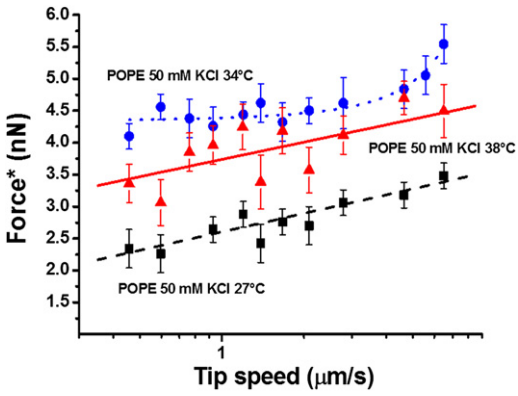

FIGURE 3 Most probable jump-through force as a function of tip speed for a POPE bilayer with coupled leaflets. The three sequences of data were obtained at 27° (*squares*) (on liquid-disordered domains in the phase transition region), at 34°C (*circles*) and 38°C (*triangles*). The dotted line for the data at 34°C is a guide for the eye, whereas the continuous and dashed lines are linear fits to the data. The lines are guides to the eye. Spring constant of the cantilever: 0.07 ± 0.02 N/m.

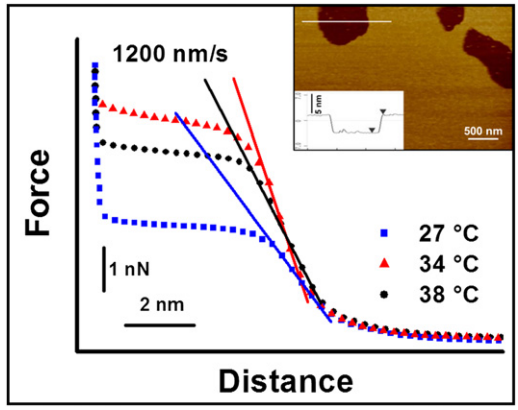

FIGURE 4 Force curves obtained on a POPE supported bilayer as a function of temperature at a constant tip speed of 1200 nm/s. Each reported curve is an average of >200 force curves. The overlaid lines highlight the steepness of the contact region between the tip and the bilayer as an indication of the bilayer deformability. Inset: AFM image of a POPE supported bilayer with a defect that allows one to measure the bilayer height. The cross section shown in the lower part of the inset corresponds to the horizontal line shown in the image.

The feature is 5.4 ± 0.3 nm. Considering the slope of the contact region between the tip and the bilayer, it is evident that when the temperature is changed from 38°C to 34°C, the elastic constant associated with the bilayer deformation increases, as marked by an increased steepness of the contact region of the force curve. However, at 27°C (i.e., in the transition state of the bilayer), the elastic constant undergoes a significant decrease. This behavior establishes that in the still liquid-disordered regions of the bilayer, not only does the jump-through force value decrease, but also the elastic constants of the bilayer at the nanoscale soften.

It is usually assumed that the viscous contribution is negligible in force spectroscopy measurements on SLB (38). In the Supporting Material, we compare the force curves acquired at different tip speeds for the three investigated temperatures to elucidate the possible contribution of viscous effects.

We also studied the dependence of the most probable jump-through force versus *log*(loading rate) on the cantilever spring constant value. In Fig. 5 *a*, the most probable jump-through force value measured on the same sample at different loading rates and with two cantilevers having different spring constants is reported. It is evident that in the case of the cantilever with a spring constant of 0.22 N/m, in the low-force-loading region, an almost constant value for the most probable jump-through force is found. Conversely, this is not the case when using the $k = 0.08$ N/m cantilever. Moreover, for the same loading rates, the cantilever with the higher spring constant shows a higher value for the jump-through force. We note, however, that a quantitative comparison between different tips is not completely feasible because the geometric shape of the tip could determine the force required to jump through the

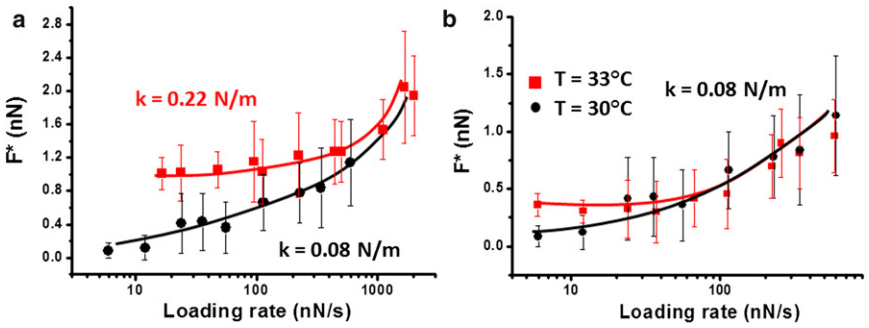

FIGURE 5 (*a*) Most probable jump-through force as a function of the loading rate on a POPE bilayer obtained with two cantilevers of different spring constants (*squares*: $k = 0.22$ N/m; *circles*: $k = 0.08$ N/m) ($T = 30°C$). (*b*) Most probable jump-through force as a function of the loading rate on the same POPE bilayer in panel *a*, obtained at two different temperatures (spring constant = 0.08 N/m). All of the continuous lines are guides to the eye.

bilayer. In Fig. 5 *b*, the data obtained with the cantilever of lower spring constant on the same POPE bilayer as in Fig. 5 *a* for two different temperatures (30°C and 33°C) are reported. Even in this case, an almost constant value for the jump-through force is obtained at 33°C for low force loading rates, which is at variance with the results obtained at 30°C.

DISCUSSION

In this work, we used atomic force spectroscopy to unravel the details of the mechanical properties of SLBs. One particular aspect of this investigation is the possibility of observing two jump-through events across a single lipid bilayer depending on the specific preparation procedure for the bilayer. Several pieces of evidence indicate that the presence of two jumps can in this case be attributed to the sequential penetration of the two leaflets: 1) In some cases, it is possible to switch reversibly from a single jump to two jumps simply by changing the tip speed (Fig. 1 *d*). 2) The overall jump distance obtained by summing up the two jumps in the above case is similar to the distance of the single jump case. 3) The appearance of one or two steps in the punch-through phenomenon is strictly dependent on the coupling between the two leaflets. If the two leaflets are coupled, only one jump-through event is observed, whereas in the case of uncoupled leaflets, two events can be observed. The first jump in the sequential penetration of the two leaflets is most likely due to the distal leaflet. This is mainly because the distal leaflet has a lower lipid density with respect to the proximal one (20), and the punch-through force value increases with lipid density in the leaflet (39). These considerations are related to the phospholipid rearrangement mechanism that is involved in the tip penetration process. In fact, we can envisage at least two cases: a penetration that mainly involves a lateral sliding of phospholipids, and a penetration that involves a compression of the lipid bilayer and a lipid rearrangement similar to the formation of a lipid pore. In the first case, the force curve behavior is mainly determined by the lateral lipid area stretching modulus. In the second case, both compression and the area stretching modulus will be involved (see Fig. S3). Fig. 1 *d* shows that the appearance of only one jump-through event or two events on POPG bilayer with uncoupled leaflets depends on the tip speed. At low speed, penetration occurs in two steps (the plot in Fig. 1 *d* reports the force value of a single penetration), the first of which is most likely due to the distal leaflet. At higher speed, only one penetration event is present, and the jump distance associates this jump-through event with the penetration across the full bilayer. A possible explanation is that a higher tip speed involves a faster slipping of one monolayer relative to the other. The increased slipping speed could result in increased friction force between the two leaflets, leading to a coupled movement of the two leaflets and a higher jump-through force. This scenario bears an important biological consequence because it is related to the possibility that the application of forces with different rates to the lipid bilayer could differently affect the activity of embedded integral membrane proteins that bear mechanosensitive domains in just one of the two leaflets (40). For example, the application of tension ramps to a micropipette-clamped lipid bilayer usually involves an instantaneous transmission of the tension to the lipid leaflet that is directly clamped by the pipette (41). The transmission of the same tension to the other leaflet could be related to the rate of the tension ramp and the degree of interleaflet coupling. In fact, previous experimental results show that interdigitation, one of the possible coupling mechanisms for lipid leaflets, can be relevant in phenomena such as the flow of one leaflet over the other, even in the case of chains with no difference in length (34). It has been demonstrated that a big difference in the surface density of lipids in the two leaflets is strongly correlated with a decreased friction in the relative flow between the leaflets. This phenomenon can be intuitively associated with an interdigitation of the final portion of the chains, which is lower in the case of a large difference in density between the two leaflets.

The possibility of observing two jump-through events increases as the lipid bilayer approaches its phase transition temperature. Fig. 2 shows that by decreasing the temperature to 24°C for a POPG SLB, it is possible to switch from a single jump-through event to the presence of two events. The bilayer at 24°C is near its phase transition,

and it is possible that fluctuations in the bilayer continuously shift the membrane from a coupled to an uncoupled state. The characteristic fluctuations rationalize the two possible cases of only one or two penetration events. The presence of a phase transition could in fact favor the uncoupling of the two leaflets. An interesting aspect of this case is that the jump-through force for the coupled leaflets penetration is about twice the value for the penetration of a single leaflet. This behavior would suggest the presence of two similar barriers that must be overcome. The two barriers could be arranged in a series or in a parallel configuration. In the parallel configuration, the force required to penetrate the system would be twice that required for the series configuration.

Fig. 2 *c* shows that the force curves on the POPG bilayers, which are characterized by two penetration events, also present an increased repulsive force when the tip approaches the bilayer surface. It is well known that all phospholipids, even zwitterionic ones, present a net surface charge when organized in a lipid bilayer. The surface of silicon nitride AFM tips is negatively charged in liquid. As a consequence, for a negatively charged lipid bilayer, an electrostatic repulsion force establishes when the two surfaces are close to each other. Upon a phase transition of the lipid bilayer/monolayer from a liquid-disordered phase to a solid-ordered one, the lateral area per lipid decreases by ~25%. Consequently, the lipid density and the surface charge density increase. The latter parameter again determines the electric field and the repulsion force. This explains why the electrostatic repulsion increases when the tip approaches a bilayer undergoing a phase transition to the solid phase.

The penetration mechanism of an AFM tip through an SLB has already been successfully connected to the spontaneous formation of lipid pores (hydrophilic or hydrophobic) (12). Most likely, the penetration of an AFM tip in an SLB involves the formation of a larger hole with respect to the spontaneous formation of a lipid pore in an unsupported lipid bilayer. The connection results from considering the role that fluctuations have with respect to the formation of a hole. In the literature, the tip penetration process has been successfully described by an energy landscape that includes two equilibrium states separated by an activation energy (12). This consideration prompts the exploitation of DFS to try to shed light on the energy landscape that describes the jump-through process in an SLB. An analogous process was studied in the case of experiments on lipid bilayer failure under the application of a tension ramp in the plane of the membrane (42). Here, we performed jump-through experiments on SLBs at different loading rates and tried to interpret the data on the basis of different theories developed for DFS.

Without considering any analytical details of the energy landscape, a monotonically increasing value of the jump-through force versus *log*(tip speed) is to be expected. This consideration is based on the assumption of a random walk of the system on the potential energy surface describing the rising over the activation energy barrier, and on the time allowed to the system for the landscape exploration. In Fig. 3 we show that the most probable jump-through force value increases with *log*(tip speed). The measurement performed at 38°C shows a linear increase of the most probable jump-through force with the *log*(tip speed). The observed trend at 38°C suggests that the process under investigation could be described by a model in which the energy barrier for the tip penetration decreases linearly with compression force. The phenomenological Bell-Evans model, which is based on the fact that the reaction rate constant depends exponentially on the applied force multiplied by the distance between the initial state and the transition state, foresees a linear dependence for the above relation. Obviously, the most critical experimental drawback is the limited tip speed range that can be explored to distinguish between different analytical dependences. We then changed the temperature to 34°C. In this case, the relation between the most probable jump-through force and the logarithm of the tip speed is not linear over the explored range. Typically, in the context of the Bell-Evans model, the presence of a change in the slope of the plot representing a rupture force versus *log*(tip speed) is interpreted as being due to the existence of more than one activation barrier. In this framework, pore formation in unsupported lipid bilayers has been described as a two-step process in which the first barrier is connected to the spontaneous generation of a pore by fluctuations (related to defects) and the second one accounts for the eventual evolution to an unstable pore (43,44). This mechanism has been exploited to explain experiments on lipid bilayer failure under the application of a tension ramp in which the presence of two different linear regimes in the F-versus-*log*(tip speed) plot was found (40). In fact, at fast loading rates, the limiting factor is supposed to be the formation of defects in the bilayer (the inner barrier), whereas at slow rates, the limiting factor is supposed to be the crossing of the critical pore diameter during the lifetime of the defect (the outer barrier). Considering the results obtained at 34°C, we can state that our experimental results, obtained by the application of a stress perpendicular to the bilayer plane, are qualitatively similar to those obtained by Evans et al. (42). Moreover, Evans et al. pointed out that for shorter alkyl chains, the defect formation frequency at constant temperature increases and, as a consequence, the region of low dependence of rupture force on loading rate expands to higher rates. Our experiments seem to suggest that by changing the mechanical properties of the bilayer according to a variation in temperature, we are able to simulate an enlargement of the effective tip speed range. The Bell-Evans model can be applied to the different linear regimes to extract k_{off}^0 and the distance to the transition state along the pushing coordinate (Δx), where k_{off}^0 represents the rate for the event

(in this case, collapse of a lipid bilayer) to occur in the absence of force. For lipid bilayers, it is connected to the probability of hole formation, in the absence of applied force, where the hole is large enough to allow tip penetration (see Supporting Material for details). It is to be stressed that previous works in the literature exploited the Bell-Evans model to infer values for the energy landscape involving the rupture or fusion events in lipid bilayer induced by applying a force with an AFM tip (16,45). Butt and Franz (12) developed specific models to describe the process of AFM tip penetration through SLBs. The models predict specific behaviors both for the jump-through force distribution at a specific tip speed and for the trend of the most probable jump-through force as a function of the *log*(tip speed). With respect to the phenomenological model, the models developed by Butt and Franz introduce specific conditions for the sample (in this case, the lipid bilayer) that allow one to extract the activation energy for tip penetration. In the Supporting Material we discuss the application of different models to our experimental data.

The relevance of the mechanical properties of the lipid bilayer for determining the jump-through force versus *log*(tip speed) relation is further confirmed by the measurement obtained at 27°C on the same POPE bilayer. At 27°C, where the bilayer is in the phase transition region and undergoes a softening behavior, the above relation is again linear.

Fig. 4 shows that the elastic portion of the force curves also undergoes a significant variation with temperature. In particular, in the phase transition region, the contact region is more compliant than it is at higher temperatures out of the transition region. By applying a model developed by Das et al. (38), we were able to fit the initial elastic contact region of the curves by an analytical function to extract the area stretching modulus of the bilayer (see Fig. S4). We obtained the following values: 0.14 N/m at 38°C, 0.16 N/m at 34°C, and 0.12 N/m at 27°C. However, in AFM measurements, we cannot exclude a possible contribution from the compression modulus. In general, given the substantially constant volume of lipid bilayers, it is very difficult to determine the possible deformation modes of the bilayer separately. Our analysis of the possible viscous contributions (Fig. S5) shows that, depending on the temperature, a viscoelastic contribution in the force curves on SLBs cannot be excluded. Moreover, considering the presence of viscous effects and the corresponding analysis of Fig. 3 for the three different temperatures, it seems that a deviation from a linear relation between the most probable jump-through force and the *log*(tip speed) occurs when the viscous effects are more prominent. The Bell model is valid only for weak pulling conditions. It is possible that in the presence of a strongly damped system, where viscoelastic effects are evident, the Bell-Evans model is no longer valid (27). In this context, many theoretical works have discussed the interpretation of the appearance of a nonlinear relation between the most probable (or average) breaking force and the *log*(tip speed). Besides the interpretation based on the presence of more than one energy barrier in the energy landscape according to the Bell model, another analysis based on Langevin dynamics demonstrated the presence of different regimes even in the presence of only one energy barrier. In particular, in the DHS model, we can obtain an analytical solution for some specific analytical functions that describe the energy landscape. We can then tentatively fit the DHS theory to our data to obtain the activation energy, the rate of the reaction at zero force, and the distance to the transition state (Fig. S6). Here, the change in temperature modifies the mechanical stability of the system and allows us to probe an enlarged effective loading rate range. Another fundamental aspect of the phenomenological model is that the relation between the rupture force and the *log*(tip speed) depends on the product of the speed with the spring constant of the pulling or pushing device. This result is a consequence of assuming a very soft device. Both theories and experiments have shown that this assumption is not always satisfied (46). In our case, if we consider the spring constants obtained for the POPE SLB and the cantilever spring constant, we must admit that they are comparable. Moreover, the phenomenological model neglects the possibility of rebinding during the rupturing attempts. The possibility of rebinding becomes relevant if a device with a high spring constant is operated at low speed (47). We therefore studied the behavior of the same POPE supported bilayer with two cantilevers endowed with different spring constants. The results of Fig. 5 *a* show that the jump-through force values obtained for the two cantilevers are different. However, the observed quantitative difference is not to be considered as being entirely due to the different spring constants, because the shape of the indenting tip could be relevant as well. However, from a qualitative point of view, Fig. 5 *a* shows that in the case of the cantilever with the higher spring constant, in the low loading rate range an almost constant value for the jump-through force is obtained. In the same loading rate region, a plateau for the jump-through force is not obtained for the softer cantilever. The presence of a plateau is usually considered as a marker of the rebinding phenomenon (47). At high loading rates, the qualitative behavior of the two cantilevers becomes comparable. In Fig. 5 *b*, we show the data obtained with the softer cantilever on the same POPE bilayer at two different temperatures. In this case, the low change in the mechanical properties of the bilayer induced by the different temperatures in the jump-through force versus *log*(loading rate) is more evident at low loading rates. The obtained results could be interpreted in the context of the comparison between the molecular and device spring constants. When the temperature decreases, the lipid bilayer becomes stiffer, and, in the comparison between the molecular and the cantilever spring constant, it is equivalent to a softer cantilever.

CONCLUSIONS

Here, we used force spectroscopy to study SLBs prepared according to different procedures. We have shown that, depending on the interleaflet coupling obtained with the preparation strategy for the SLB, the force curves on the bilayer can show one or two penetration events. In fact, for uncoupled leaflets, the tip penetrates sequentially through the two leaflets, whereas in the case of coupled leaflets, the jump of the AFM tip through the bilayer occurs in only one step. Moreover, we found that the characteristic jump-through force value on SLBs depends on the cantilever speed, as in DFS experiments performed on other systems. We therefore tried to apply theoretical models developed in the context of DFS to our cases, and we discussed the obtained results. We also found that the studied model system is suitable for examining other relevant aspects raised in the context of DFS. In particular, we showed how the temperature or the spring constant of the cantilever might be exploited to extend the effective loading rate range to more reliably fit the theoretical models to the experimental data. We observed deviations from the Bell-Evans phenomenological model that can be rationalized in terms of other theories.

SUPPORTING MATERIAL

Seven sections, eight figures, and references (48–52) are available at http://www.biophysj.org/biophysj/supplemental/S0006-3495(12)00619-4.

We thank Dr. Marco Pieruccini for a critical reading of the manuscript.

This work was supported by the Ministry of Education, Universities and Research/Fund for Investing in Fundamental Research (Italnanonet).

REFERENCES

1. Sackmann, E. 1996. Supported membranes: scientific and practical applications. *Science.* 271:43–48.
2. Tamm, L. K., and H. M. McConnell. 1985. Supported phospholipid bilayers. *Biophys. J.* 47:105–113.
3. Alessandrini, A., and P. Facci. 2011. Unraveling lipid/protein interaction in model lipid bilayers by atomic force microscopy. *J. Mol. Recognit.* 24:387–396.
4. Alessandrini, A., H. M. Seeger, …, P. Facci. 2011. What do we really measure in AFM punch-through experiments on supported lipid bilayers? *Soft Matter.* 7:7054–7064.
5. Alessandrini, A., and P. Facci. 2005. AFM: a versatile tool in biophysics. *Meas. Sci. Technol.* 16:R65–R92.
6. Picas, L., F. Rico, and S. Scheuring. 2012. Direct measurement of the mechanical properties of lipid phases in supported bilayers. *Biophys. J.* 102:L01–L03.
7. Dufrêne, Y. F., T. Boland, …, G. U. Lee. 1998. Characterization of the physical properties of model biomembranes at the nanometer scale with the atomic force microscope. *Faraday Discuss.* 111:79–94, discussion 137–157.
8. Garcia-Manyes, S., and F. Sanz. 2010. Nanomechanics of lipid bilayers by force spectroscopy with AFM: a perspective. *Biochim. Biophys. Acta.* 1798:741–749.
9. Garcia-Manyes, S., L. Redondo-Morata, …, F. Sanz. 2010. Nanomechanics of lipid bilayers: heads or tails? *J. Am. Chem. Soc.* 132:12874–12886.
10. Garcia-Manyes, S., G. Oncins, and F. Sanz. 2005. Effect of temperature on the nanomechanics of lipid bilayers studied by force spectroscopy. *Biophys. J.* 89:4261–4274.
11. Loi, S., G. Sun, …, H. J. Butt. 2002. Rupture of molecular thin films observed in atomic force microscopy. II. Experiment. *Phys. Rev. E.* 66:031602.
12. Butt, H. J., and V. Franz. 2002. Rupture of molecular thin films observed in atomic force microscopy. I. Theory. *Phys. Rev. E.* 66:031601.
13. Evans, E., and K. Ritchie. 1997. Dynamic strength of molecular adhesion bonds. *Biophys. J.* 72:1541–1555.
14. Evans, E. 2001. Probing the relation between force—lifetime—and chemistry in single molecular bonds. *Annu. Rev. Biophys. Biomol. Struct.* 30:105–128.
15. Sullan, R. M., J. K. Li, …, S. Zou. 2010. Cholesterol-dependent nanomechanical stability of phase-segregated multicomponent lipid bilayers. *Biophys. J.* 99:507–516.
16. Abdulreda, M. H., and V. T. Moy. 2007. Atomic force microscope studies of the fusion of floating lipid bilayers. *Biophys. J.* 92:4369–4378.
17. Keller, D., N. B. Larsen, …, O. G. Mouritsen. 2005. Decoupled phase transitions and grain-boundary melting in supported phospholipid bilayers. *Phys. Rev. Lett.* 94:025701.
18. Seeger, H. M., G. Marino, …, P. Facci. 2009. Effect of physical parameters on the main phase transition of supported lipid bilayers. *Biophys. J.* 97:1067–1076.
19. Xing, C., and R. Faller. 2008. Interactions of lipid bilayers with supports: a coarse-grained molecular simulation study. *J. Phys. Chem. B.* 112:7086–7094.
20. Xing, C., and R. Faller. 2009. Density imbalances and free energy of lipid transfer in supported lipid bilayers. *J. Chem. Phys.* 131:175104.
21. Collins, M. D. 2008. Interleaflet coupling mechanisms in bilayers of lipids and cholesterol. *Biophys. J.* 94:L32–L34.
22. Collins, M. D., and S. L. Keller. 2008. Tuning lipid mixtures to induce or suppress domain formation across leaflets of unsupported asymmetric bilayers. *Proc. Natl. Acad. Sci. USA.* 105:124–128.
23. Charrier, A., and F. Thibaudau. 2005. Main phase transitions in supported lipid single-bilayer. *Biophys. J.* 89:1094–1101.
24. Leonenko, Z. V., E. Finot, …, D. T. Cramb. 2004. Investigation of temperature-induced phase transitions in DOPC and DPPC phospholipid bilayers using temperature-controlled scanning force microscopy. *Biophys. J.* 86:3783–3793.
25. Franz, V., S. Loi, …, H. J. Butt. 2002. Tip penetration through lipid bilayers in atomic force microscopy. *Colloids Surf. B Biointerfaces.* 23: 191–200(10).
26. Bell, G. I. 1978. Models for the specific adhesion of cells to cells. *Science.* 200:618–627.
27. Dudko, O. K., A. E. Filippov, …, M. Urbakh. 2003. Beyond the conventional description of dynamic force spectroscopy of adhesion bonds. *Proc. Natl. Acad. Sci. USA.* 100: 378–81.
28. Merkel, R., P. Nassoy, …, E. Evans. 1999. Energy landscapes of receptor-ligand bonds explored with dynamic force spectroscopy. *Nature.* 397:50–53.
29. Dudko, O. K., G. Hummer, and A. Szabo. 2006. Intrinsic rates and activation free energies from single-molecule pulling experiments. *Phys. Rev. Lett.* 96:108101.
30. Hummer, G., and A. Szabo. 2003. Kinetics from nonequilibrium single-molecule pulling experiments. *Biophys. J.* 85:5–15.
31. Bartolo, D., I. Derényi, and A. Ajdari. 2002. Dynamic response of adhesion complexes: beyond the single-path picture. *Phys. Rev. E.* 65:051910.

32. Seeger, H. M., A. Di Cerbo, …, P. Facci. 2010. Supported lipid bilayers on mica and silicon oxide: comparison of the main phase transition behavior. *J. Phys. Chem. B.* 114:8926–8933.

33. Israelachvili, J. 1992. Intermolecular and Surface Forces. Academic Press, New York.

34. Merkel, R., E. Sackmann, and E. Evans. 1989. Molecular friction and epitactic coupling between monolayers in supported bilayers. *J. Phys. (Paris).* 50:1535–1555.

35. Cook, S. M., T. E. Schäffer, …, K. M. Lang. 2006. Practical implementation of dynamic methods for measuring atomic force microscope cantilever spring constants. *Nanotechnology.* 17:2135–2145.

36. Pera, I., R. Stark, …, F. Benfenati. 2004. Using the atomic force microscope to study the interaction between two solid supported lipid bilayers and the influence of synapsin I. *Biophys. J.* 87:2446–2455.

37. Heimburg, T. 1998. Mechanical aspects of membrane thermodynamics. Estimation of the mechanical properties of lipid membranes close to the chain melting transition from calorimetry. *Biochim. Biophys. Acta.* 1415:147–162.

38. Das, C., K. H. Sheikh, …, S. D. Connell. 2010. Nanoscale mechanical probing of supported lipid bilayers with atomic force microscopy. *Phys. Rev. E.* 82:041920.

39. Grant, L. M., and F. Tiberg. 2002. Normal and lateral forces between lipid covered solids in solution: correlation with layer packing and structure. *Biophys. J.* 82:1373–1385.

40. Sachs, F. 2010. Stretch-activated ion channels: what are they? *Physiology (Bethesda).* 25:50–56.

41. Mukhin, S. I., and S. V. Baoukina. 2004. Inter-layer slide and stress relaxation in a bilayer lipid membrane in the patch-clamp setting. *Biol. Membrany.* 21:506–517.

42. Evans, E., V. Heinrich, …, W. Rawicz. 2003. Dynamic tension spectroscopy and strength of biomembranes. *Biophys. J.* 85:2342–2350.

43. Glaser, R. W., S. L. Leikin, …, A. I. Sokirko. 1988. Reversible electrical breakdown of lipid bilayers: formation and evolution of pores. *Biochim. Biophys. Acta.* 940:275–287.

44. Fuertes, G., D. Giménez, …, J. Salgado. 2011. A lipocentric view of peptide-induced pores. *Eur. Biophys. J.* 40:399–415.

45. Hager-Barnard, E. A., and N. A. Melosh. 2010. Effects of tip-induced material reorganization in dynamic force spectroscopy. *Phys. Rev. E.* 82:031911.

46. Maitra, A., and G. Arya. 2010. Model accounting for the effects of pulling-device stiffness in the analyses of single-molecule force measurements. *Phys. Rev. Lett.* 104:108301.

47. Friddle, R. W., P. Podsiadlo, …, A. Noy. 2008. Near-equilibrium chemical force microscopy. *J. Phys. Chem. C.* 112:4986–4990.

48. Fraxedas, J., S. Garcia-Manyes, …, F. Sanz. 2002. Nanoindentation: toward the sensing of atomic interactions. *Proc. Natl. Acad. Sci. USA.* 99:5228–5232.

49. Garcia-Manyes, S., G. Oncins, and F. Sanz. 2005. Effect of ion-binding and chemical phospholipid structure on the nanomechanics of lipid bilayers studied by force spectroscopy. *Biophys. J.* 89:1812–1826.

50. Cappella, B., and G. Dietler. 1999. Force-distance curves by atomic force microscopy. *Surf. Sci. Rep.* 34:1–104.

51. Best, R. B., E. Paci, …, O. K. Dudko. 2008. Pulling direction as a reaction coordinate for the mechanical unfolding of single molecules. *J. Phys. Chem. B.* 112:5968–5976.

52. Williams, P. M. 2003. Analytical descriptions of dynamic force spectroscopy: behaviour of multiple connections. *Anal. Chim. Acta.* 479:107–115.